catalysts

MDPI

Article

Metals on ZrO_2: Catalysts for the Aldol Condensation of Methyl Ethyl Ketone (MEK) to C_8 Ketones

Zahraa Al-Auda [1,2], Hayder Al-Atabi [1,2] and Keith L. Hohn [1,*]

[1] Department of Chemical Engineering, Kansas State University, 1005 Durland Hall, Manhattan, KS 66506, USA; alauda@ksu.edu (Z.A.-A.); alatabi@ksu.edu (H.A.-A.)
[2] Department of Chemical Engineering, The University of Technology, Baghdad, Iraq
* Correspondence: hohn@ksu.edu; Fax: +1-785-532-7372

Received: 1 October 2018; Accepted: 30 November 2018; Published: 5 December 2018

Abstract: Methyl ethyl ketone (MEK) was converted to heavier ketones in one step, using a multi-functional catalyst having both aldol condensation (aldolization and dehydration) and hydrogenation properties. 15% Cu supported zirconia (ZrO_2) was investigated in the catalytic gas phase reaction of MEK in a fixed bed reactor. The results showed that the main product was 5-methyl-3-heptanone (C_8 ketone), with side products including 5-methyl-3-heptanol, 2-butanol, and other heavy products (C_{12} and up). The effects of various reaction parameters, like temperature and molar ratio of reactants (H_2/MEK), on the overall product selectivity were studied. It was found that with increasing the temperature of the reaction, the selectivity to the C_8 ketone increased, while selectivity to the 2-butanol decreased. Also, hydrogen pressure played a significant role in the selectivity of the products. It was observed that with increasing the H_2/MEK molar ratio, the 2-butanol selectivity increased because of the hydrogenation reaction, while decreasing this ratio led to increasing the aldol condensation products. In addition, it was noted that both the conversion and selectivity to the main product increased using a low loading percentage of copper, 1% Cu–ZrO_2. The highest selectivity of 5-methyl-3-heptanone reached ~64%, and was obtained at a temperature of around 180 °C and a molar ratio of H_2/MEK equal to 2. Other metals (Ni, Pd, and Pt) that were supported on ZrO_2 also produced 5-methyl-3-heptanone as the main product, with slight differences in selectivity, suggesting that a hydrogenation catalyst is important for producing the C_8 ketone, but that the exact identity of the metal is less important.

Keywords: methyl ethyl ketone; heavier ketone; aldol condensation reaction; copper; zirconia

1. Introduction

With declining petroleum resources, more attention has been paid to developing biomass as a sustainable source of renewable fuels and chemicals. In general, the aldol condensation reaction is considered as one of the most powerful C–C bond forming reactions [1] to form large organic molecules. In the fine chemical industry, the base–catalyzed aldol condensation is a common method of coupling organic molecules [2]. The C–C bond formation proceeds via condensation between a molecule containing a carbonyl group and another molecule containing an activated methylenic group, under suitable operating conditions [3]. Aldol condensations involve reactions forming β-hydroxy aldehydes (β-aldol) or β-hydroxy ketone (β-ketol), either by self-condensations or mixed condensations of aldehydes and ketones. Then, via the dehydration of the intermediate β-aldol or β-ketol, α,β-unsaturated aldehydes or α,β-unsaturated ketones are formed [4]. Finally, further hydrogenation yields heavier aldehydes or heavier ketones. In fact, the aldol condensation reactions are commercially significant in the production of the intermediates needed to produce other commercially important products.

The largest volume aldol reaction product of acetone is methyl isobutyl ketone (MIBK), which is an excellent solvent for cellulose, vinyl, epoxy, and acrylic resins, in addition to resin-based coating systems [5]. Industrially, MIBK is manufactured in the following three steps: (i) an aldolization reaction of acetone to produce diacetone alcohol (DAA); (ii) the dehydration of DAA to mesityl oxide (MO); and (iii) the hydrogenation of the olefin double bond of MO to give MIBK [6].

These processes are intricate and require high operating costs, so recently, a one-step process to convert acetone to MIBK has become commercially possible. Reichle [7] described the condensation of aldehydes and ketones in the gas phase, especially acetone over catalysts consisting of lithium ions supported on a complex magnesium–aluminum oxide–hydroxide mixture. The reactions formed iso-phorone and mesityl oxide with isophorone/mesityl oxide ratios > 1. Kelly [5] studied the aldol condensation reaction of acetone over two beds of catalysts consisting of 3 mL of the K–SiO_2 catalyst, followed by a 3 mL bed of a hydrogenation catalyst consisting of 1% palladium supported on carbon. The main product was MIBK, in addition to mesityl oxide and isophorone. He also investigated the aldol condensation of methyl ethyl ketone (MEK) over different catalysts. He reported that, using Na–SiO_2 and Cs–SiO_2, the major product was an α,β-unsaturated ketone (5-methyl-4-hepten-3-one), with both isomers (*Z* and *E*) being formed at temperatures between 325 and 400 °C. He further tested the aldol condensation of MEK over two beds comprised of Na–SiO_2 and Cu–Zn. The main products were 5-methyl-3-heptanone and 5-methyl-3-heptanol, which result in the subsequent hydrogenation of an α,β-unsaturated ketone. However, over just one bed consisting of Cu–Zn alone, the main product was believed to be bicyclo-[3,3,0]-octane-3,7-dione, resulting from a dehydrogenation reaction of two molecules of MEK, with little evidence of aldol condensation compounds.

It is comparatively easy to hydrogenate α,β-unsaturated carbonyls into saturated carbonyls, rather than into unsaturated alcohols [8–10], as thermodynamics favor the hydrogenation of C=C bonds over C=O bonds [11,12]. For kinetic reasons, the reactivity of the C=C bond for hydrogenation is higher than the C=O bond, leading to saturated aldehydes or saturated alcohols via the sequential hydrogenation of the aldehydes over conventional supported hydrogenation catalysts (Pt, Ru, Ni, etc.) [12]. The catalysts used for the hydrogenation of double bonds in α,β-unsaturated ketones can be divided into two groups—one that includes platinum metals as a main component or a modifier, and the other group consisting of Ni, Cu, or Co [13]. Cu catalysts are more selective for the hydrogenation of the C=C bond rather than the C=O bond, when used in the reduction of α,β-unsaturated carbonyls [11].

Szöllősi, et al. [14] carried out comparative studies to determine the activity and selectivity for the gas-phase hydrogenation of 3-penten-2-one to form 2-pentanone on well-defined SiO_2 (Cab-O-Sil)-supported metals (Ni, Cu, Ru, Rh, Pd, and Pt). The activity of the metals investigated in the hydrogenation of 3-penten-2-one followed the order of Pt > Pd > Rh >> Ru > Ni > Cu at 393 K, and Pt > Pd > Rh > Ru-Ni >> Cu at 473 K. However, Ravasio, Nicoletta et al. [15] reported that Cu–Al_2O_3 is an effective catalyst for the selective reduction of different α,β-unsaturated carbonyl compounds. Ravasio, Nicoletta et al. [16] also reported that Cu–SiO_2 was selective for the hydrogenation of unsaturated ketones.

The coupling reaction of small molecules to produce large molecules is a commercially attractive method to form a range of products with specific structures and properties. For this reason, this work utilizes aldol condensation for upgrading MEK to heavier ketones. MEK is an attractive feedstock, as it can be derived from renewable resources, for example, by dehydrating 2,3 butanediol (2,3 BDO) [17–24], which can be produced at a high yield from biomass-derived sugars [25–32]. The process studied includes a single step to create C–C bonds between MEK via heterogeneous catalysis, using a multifunctional catalyst having aldol condensation (aldolization and dehydration) and hydrogenation properties, to produce a heavier ketone (C_8) in a single reactor. The main product, 5-methyl-3-heptanone, is an important intermediate used to produce heavier aliphatic alcohol (5-methyl-3-heptanol) via a hydrogenation reaction. It can also be used to produce C_8 alkenes and C_8 alkanes for use as a fuel by hydrogenation–dehydration reactions.

Our aim in this work is to develop a catalyst that can condense MEK into heavier ketones in a single step. ZrO_2 was chosen as a support, as it has both acidic and basic properties. The cooperative effect of acidic and basic sites makes ZrO_2 function as an effective catalyst [33]. It is hypothesized that the basic sites on ZrO_2 can catalyze the aldol condensation reaction, while its acidic sites are suitable for dehydration reactions [34]. Supported metals like copper have been investigated to see whether they can hydrogenate aldol condensation products (α,β-unsaturated ketones) to saturated ketones. We hypothesize that Cu/ZrO_2 will be capable of catalyzing the three steps to produce C_8 ketones from MEK. The optimizing the operating conditions, like the temperature, H_2/MEK molar ratio, and Cu loading, were studied so as to obtain the highest selectivity of 5-methyl-3-heptanone. The effect of different metals (Ni, Pd, and Pt) loaded on ZrO_2 was considered.

2. Results and Discussions

2.1. Characterization of Catalysts

2.1.1. XRD

The XRD patterns of pure ZrO_2 and calcined different metals (Cu, Ni, Pt, and Pd) over ZrO_2, in addition to the different loadings of copper on ZrO_2, are shown in Figure 1.

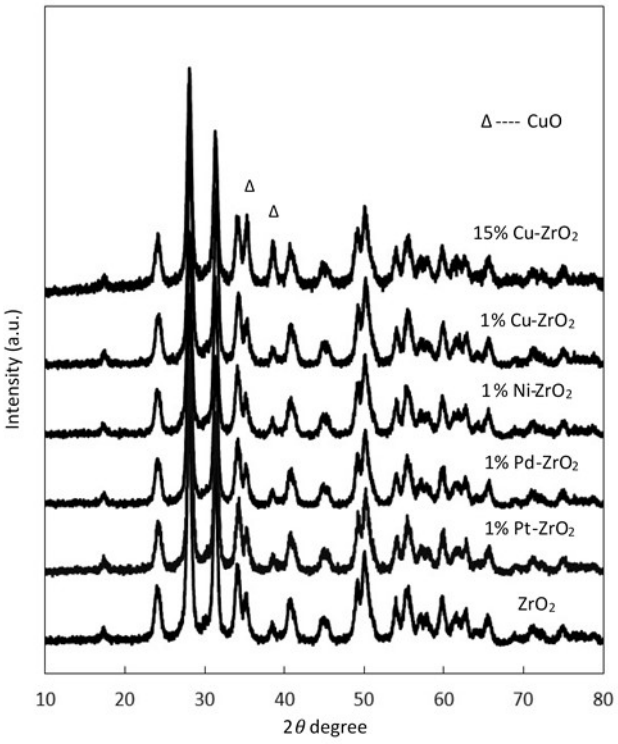

Figure 1. XRD patterns for pure ZrO_2 and different metals supported on ZrO_2.

As shown in this figure, the zirconia displays a monoclinic phase in all of the samples. ZrO_2 peaks were observed at 2θ = 24.05°, 31.47°, 35.3°, 38.5°, 40.72°, and 61.37° [JCPDS 37-1484]. No diffraction peaks for platinum or palladium oxide were detected in the diffraction profiles of 1% Pt–ZrO_2 and 1% Pd–ZrO_2, indicating that these metals have been well dispersed at low loadings on the support. Also, for 1% Ni–ZrO_2, no obvious diffraction peaks were observed for NiO, suggesting that the NiO was dispersed well on the surface of the support. For Cu–ZrO_2, there were no distinguishable diffraction peaks representing crystalline CuO at a low Cu loading (1 wt % Cu–ZrO_2), either because the copper

particles are smaller than 40 Å in size, the detection limit of XRD [35,36], or because the peaks are obscured by ZrO_2 peaks at similar diffraction angles.

For 15% Cu–ZrO_2, peaks attributed to crystalline CuO at 2θ = 35.5°, 38.7° can be distinguished from the characteristic ZrO_2 peaks near these diffraction angles, confirming the presence of CuO, as clusters at a higher loading of Cu. This is in accordance with the results obtained from the TPR measurements described below.

2.1.2. H_2-TPR

H_2-TPR measurements were performed to investigate the reducibility of the different metals (Cu, Ni, Pt, and Pd) supported over ZrO_2, and the dispersion of the metals on the support. The TPR profile provides information on the dispersion of the metal species over the support, and gives details of the interaction between the metal ions and the support [37], and it is well suited for studying systems with a high metal dispersion, whose characteristics are beyond the detectability limits of XRD [35]. Figure 2a exhibits the TPR profiles of pure ZrO_2 and Cu supported on ZrO_2. As can be seen, ZrO_2 displays no reduction peaks, while 1% Cu–ZrO_2 exhibits three reduction peaks centered at 176, 378, and 441 °C. Shimokawable et al. [38] and Dow et al. [39] studied the reduction behavior of Cu–ZrO_2 and CuO–YSZ catalysts, respectively. They elucidated that the lower temperature peaks are because of highly dispersed CuO and/or Cu^{2+} ions with an octahedral environment. Robertson et al. [40] and Van der Grift et al. [37] studied Cu–SiO_2 catalysts. These authors demonstrated that highly dispersed CuO species are more easily reduced than bulk CuO. Based on the literature data and the XRD results, it can be concluded that the first peak is attributed to highly dispersed CuO species, while the second and third peaks are assigned to the small CuO clusters with different particle sizes. For 15% Cu–ZrO_2, it can be seen that there are four peaks. The first and second peaks at low reduction temperatures (103 and 156 °C) can be ascribed to well dispersed CuO, whereas the large peaks (third and fourth) at high reduction temperatures (223 and 242 °C) are attributed to bulk CuO. A considerable shift was observed for the high temperature peaks at a high Cu loading, likely due to the weakening of the metal–support interaction. This may be because more Cu species were located on the outer surface of the support and were easily accessible, while at the lower metal loading Cu species were highly disperse and were located in the pores of the ZrO_2 support, leading to a low accessibility towards hydrogen, and a higher reduction temperature [41].

The TPR profiles of the different metals (Cu, Ni, Pt, and Pd) supported over ZrO_2 are demonstrated in Figure 2b. For the catalysts, Ni–ZrO_2 [42–44], Pd–ZrO_2 [45,46], and Pt–ZrO_2 [47], two obvious peaks were distinct, which can be attributed to the different interactions between metal oxide and the support. The first peak at the lower reduction temperatures is assigned to relatively free or superficial metal oxide on the surface of ZrO_2, and the second peak, which is at a higher reduction temperature, is attributed to metal oxide that interacts strongly with ZrO_2. The amount of H_2 consumed for the different catalysts is shown in Table 1.

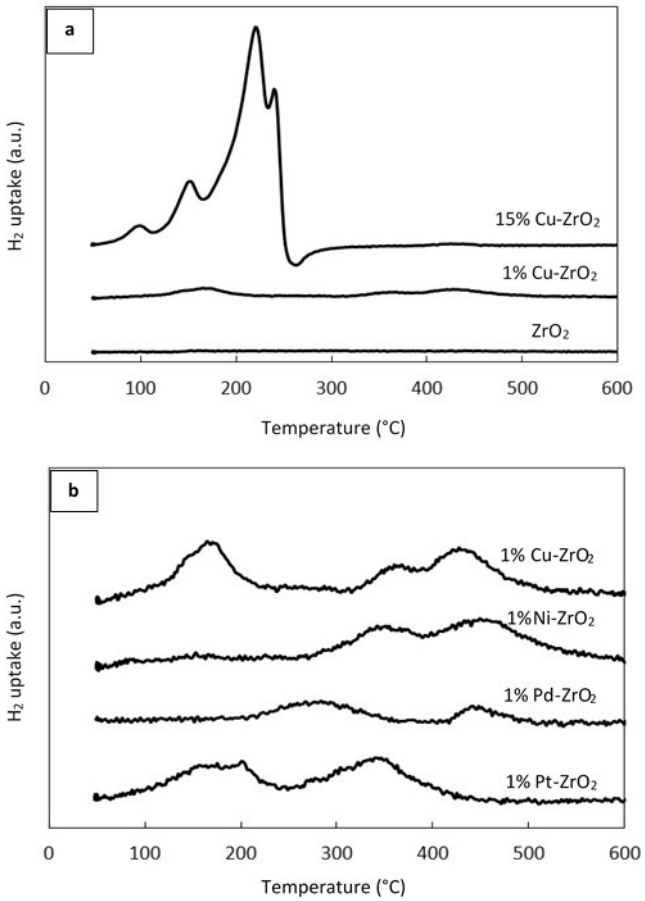

Figure 2. (**a**) H_2-TPR profiles of pure ZrO_2 and ZrO_2 loaded with different Cu percentages; (**b**) H_2-TPR profiles of different metals loaded on ZrO_2.

Table 1. Total consumption of H_2, NH_3, and CO_2 during the H_2-TPR, NH_3-TPD, and CO_2-TPD experiments for the different catalysts.

Catalyst	H_2 Uptake mmol/g	NH_3 Uptake mmol/g	CO_2 Uptake mmol/g
ZrO_2	_	0.12	0.053
15% Cu–ZrO_2	1.46	0.27	0.092
1% Cu–ZrO_2	0.17	0.17	0.075
1% Ni–ZrO_2	0.18	0.15	0.064
1% Pd–ZrO_2	0.05	0.16	0.071
1% Pt–ZrO_2	0.13	0.16	0.066

2.1.3. NH_3-TPD and CO_2-TPD

NH_3-TPD and CO_2-TPD experiments were carried out to investigate the acid–base properties of the reduced catalysts. Figure 3a shows the NH_3-TPD profile of pure ZrO_2, and the catalysts with different reduced metals (Cu, Ni, Pd, and Pt) loaded on the ZrO_2, as well as the Cu–ZrO_2 catalysts with different Cu loadings. Figure 3b displays the CO_2-TPD profile for the same catalysts.

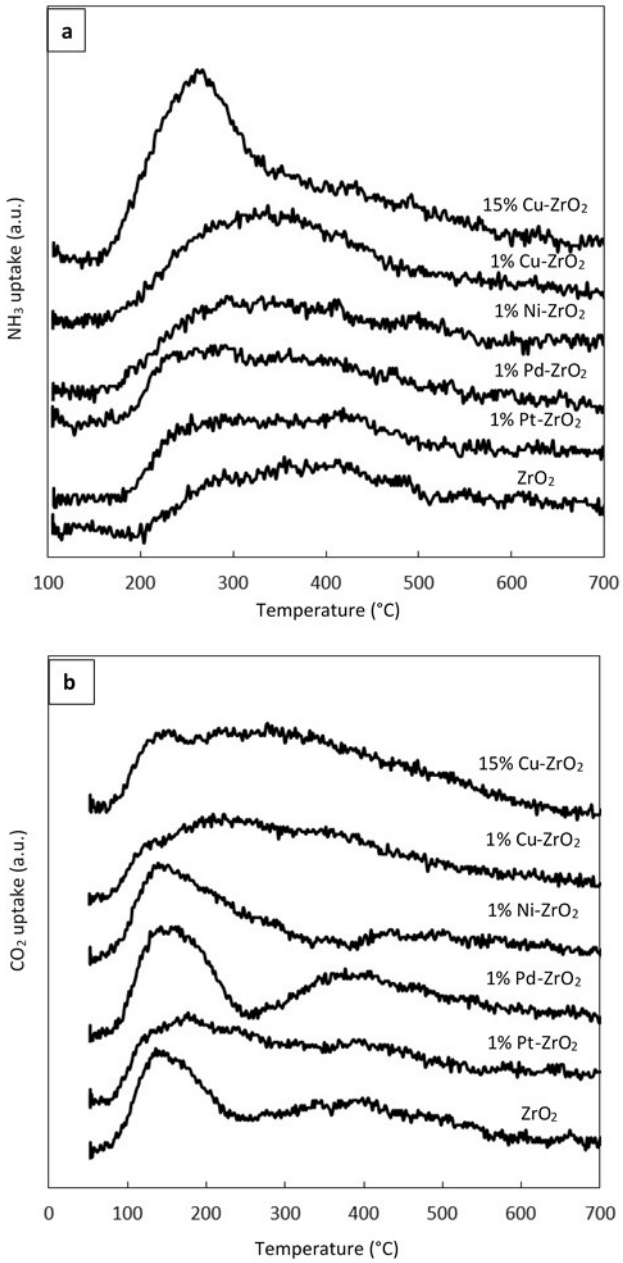

Figure 3. (**a**) NH_3-TPD profiles of different catalysts; (**b**) CO_2-TPD profiles of different catalysts.

As can be seen from Figure 3a, the broad NH_3 desorption peaks over ZrO_2 and the different supported metal catalysts at low loadings extend from 160 to 580 °C. Also, there is an obvious peak at 328 °C for 1% Cu–ZrO_2, while a sharp peak appeared at 270 °C for the 15% Cu–ZrO_2, with a broad shoulder extending out to 600 °C. For all of the supported catalysts, the amount of acid sites slightly increased, as compared to the support alone. A notable increase in the number of acid sites can be seen over 15% Cu–ZrO_2 (see Table 1).

Figure 3b shows the CO_2-TPD profiles of the different catalysts. For pure ZrO_2 and 1% Pd–ZrO_2, two obvious peaks were distinct around 143 and 393 °C, and 151 and 378 °C, respectively. The two peaks can be indicative of different base sites of varying base strength, which suggests that there are both weak and strong base sites on these catalysts. 1% Ni–ZrO_2 exhibits one clear peak around 146 °C. For the 1% Pt–ZrO_2 and 1% Cu–ZrO_2 catalysts, broad CO_2 desorption peaks appeared with a long tail that extend to higher desorption temperatures. Increasing the Cu loading percentage (15% Cu–ZrO_2) led to a split in the desorption peak forming two peaks. The number of base sites were higher for the

supported metal catalysts than for the support. The number of moles of NH_3 and CO_2 adsorbed for the different catalysts are reported in Table 1.

2.2. Catalytic Reaction of MEK to Heavier Ketones in a Fixed Bed Reactor

2.2.1. Effect of Reaction Temperature

The effect of the reaction temperature on the conversion of MEK and the selectivity of the main products over 15% Cu–ZrO_2 was investigated for a temperature range of 140 to 200 °C. Figure 4 shows the changes in the conversion of MEK and the selectivity of products with different reaction temperatures after one hour on stream. As can be seen from this figure, the conversion of MEK increased from 56% to 85% as the temperature increased from 140 to 200 °C. Also, the selectivity of the products was strongly affected by the reaction temperature. The C_8 ketone production increased to over 61% at 180 °C. Higher temperatures also led to more heavy products, including C_{12} ketones, C_{12} alcohols, and condensation products. The 2-butanol production was favored at lower temperatures, going from 75% at 140 °C to 4% at 200 °C, indicating that the activation energy for the hydrogenation of MEK to 2-butanol is lower than the activation energy for coupling reactions.

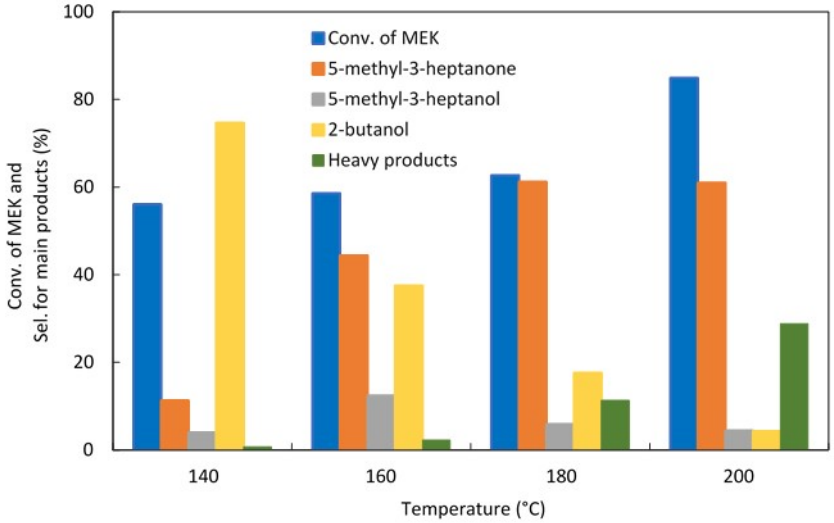

Figure 4. Catalytic results for the conversion of methyl ethyl ketone (MEK) to several products at different temperatures. Reaction conditions: catalyst weight, 1.0 g (15% Cu–ZrO_2); feed rate of MEK, 1.0 mL/h; H_2/MEK molar ratio, 2; space time, 89 g mol^{-1} h. Heavy products include C_{12} ketone, C_{12} alcohol, condensation products, and so on.

2.2.2. Effect of H_2/MEK Molar Ratio

Experiments were performed to study the effect of changing the molar ratio of H_2 to MEK on the conversion of MEK and the selectivity of products over 15% Cu–ZrO_2. The results are shown in Figure 5. Increasing the molar ratio of H_2/MEK slightly increases the conversion of MEK, but there is a significant impact on selectivity of the products with changing this ratio. It was observed that higher H_2/MEK ratios lead to increasing amounts of 2-butanol and lower amounts of C_8 ketones. This suggests that higher amounts of hydrogen change the competition between the hydrogenation and aldol condensation of MEK, leading to higher amounts of 2-butanol. Higher amounts of hydrogen also lead to the further hydrogenation of the C_8 ketone, as evidenced by the increasing conversion of the C_8 ketone to C_8 alcohol, with an increasing H_2/MEK molar ratio. With increasing the molar ratio from 2 to 15, the C_8 ketone selectivity decreased from 61% to 11%, but at H_2/MEK where the molar ratio equals 1, the amount of C_8 ketone decreased as a result of the increasing heavy products. This is

associated with increasing the 2-butanol from 4% to 76% and with increasing the H_2/MEK molar ratio from 1 to 15. Also, it was noted that the heavy product selectivity decreased with excess hydrogen.

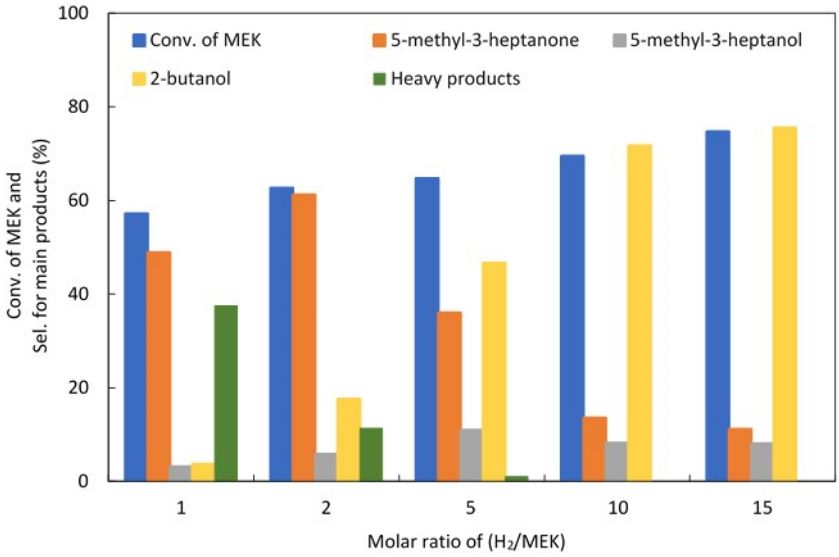

Figure 5. Catalytic results for the conversion of MEK to the main products with different H_2/MEK molar ratios. Reaction conditions: catalyst weight, 1.0 g (15% Cu–ZrO_2); feed rate of MEK, 1.0 mL/h; reaction temperature, 180 °C; space time, 89 g mol^{-1} h. Heavy products include C_{12} ketone, C_{12} alcohol, condensation products, and so on.

As seen in Figure 5, the selectivity to the C_8 ketone increased while conversion was fairly flat as the H_2/MEK ratio decreases. This begs the question of whether removing hydrogen would further improve the C_8 ketone yield. For this reason, an experiment was conducted without H_2 (H_2/MEK molar ratio = 0) (not shown in the figure). For this experiment, the MEK conversion was quite low—less than 15%. The main products that formed were condensation products, like cyclic trimers and aromatics (39%), methyl vinyl ketone (MVK) resulting from the dehydrogenation of MEK (27%), and unsaturated ketones (20%). Interestingly, the C_8 ketone was formed (13.5%) that should result from the hydrogenation of the unsaturated C_8 ketone, even though there was no hydrogen in the feed. It is hypothesized that the H_2 that was formed from the dehydrogenation of MEK to MVK was responsible for the hydrogenation reaction, which led to producing the C_8 ketone.

2.2.3. Effect of Space Time

The effect of space time (W/FA_0, where W is the weight of the catalyst (g), and FA_0 is the molar flow rate of MEK (mol h^{-1})) was evaluated in order to better understand the reaction mechanism of MEK. Figure 6 shows the change in the conversion of MEK and the distribution of products over 15% Cu–ZrO_2, with the changing of space times at a feed rate of MEK of 1 mL/h in the presence of H_2 at 180 °C after 1 h. As can been seen, the conversion of MEK increases from 47% to 74% when the space time increases from 18 to 116 g mol^{-1} h. The selectivity of the C_8 ketone increases with the increasing space time, reaching a maximum of 61% when the space time W/FA_0 was 89 g mol^{-1} h, then decreasing as the selectivity to heavy products increases. At low space times, MEK is hydrogenated to produce 2-butanol with a selectivity above 48%. The 2-butanol selectivity decreases with the increasing space time to reach about 13% at a space time of 116 g mol^{-1} h. MVK is produced as a result of the dehydrogenation of MEK at a low space time, but its selectivity decreases with the increasing space time.

The results in Figure 6 could be interpreted to imply that 2-butanol is a key intermediate in producing C_8 ketones; 2-butanol is the most prevalent product at low space times, but its selectivity decreases as the space time increases, in favor of 5-methyl-3-heptanone. It is possible that the C_8 ketone

results from the Guerbet condensation [48,49] of 2-butanol, followed by the dehydrogenation of C_8 alcohol. For these reasons, the reaction of 2-butanol on 15% Cu–ZrO_2 was carried out with different space times. As can be seen from Figure 7, the conversion of 2-butanol increases from 37% to 76% with the increasing space times from 4 to 91 g mol^{-1} h. However, the selectivity of MEK produced from the dehydrogenation of 2-butanol decreases with the increasing space times, from 87% to 53%, and is associated with increasing the C_8 ketone from 0% to 30%. This suggests that MEK is responsible for producing the C_8 ketone instead of obtaining the C_8 ketone from 2-butanol directly via Guerbet condensation. It is also important to note that at low space times, where mainly primary reactions should occur, no C_8 ketones or alcohols were detected. MVK and 2,3 BDO were detected at low space times, as a result of the dehydrogenation and hydration of MEK, respectively, and both decreased with increasing space times.

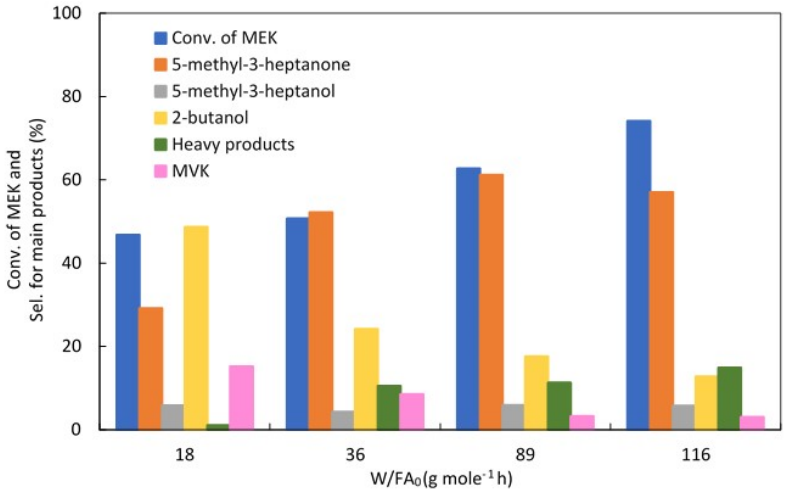

Figure 6. Catalytic results for the conversion of MEK to products with different space times after 1 h of the reaction. Reaction conditions: catalyst weight, 1.0 g (15 wt % Cu–ZrO_2); feed rate of MEK, 1.0 mL/h; H_2/MEK molar ratio, 2; reaction temperature, 180 °C. Heavy products include C_{12} ketone, C_{12} alcohol, condensation products, and so on.

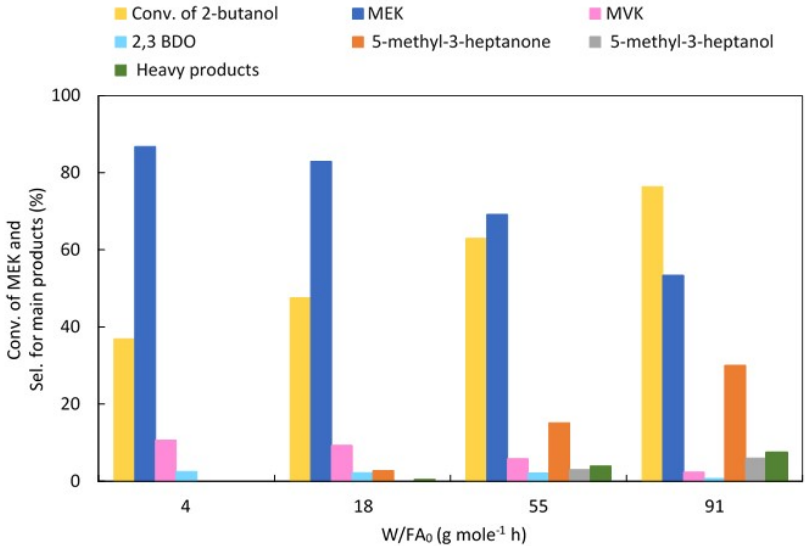

Figure 7. Catalytic results for the conversion of 2-butanol to a variety of products with different space times after 1 h of the reaction. Reaction conditions: catalyst weight, 1.0 g (15 wt % Cu–ZrO_2); feed rate of 2-butanol, 1.0 mL/h; H_2/2-butanol molar ratio, 2; reaction temperature, 180 °C. Heavy products include C_{12} ketone, C_{12} alcohol, condensation products, and so on.

2.2.4. Effect of Copper Loading on the Support

The effect of copper loading was investigated by conducting experiments with just the support (ZrO_2), and with copper supported on it at high and low loadings (15% and 1%). Table 2 shows that only minor amounts of the C_8 ketone were obtained from the MEK condensation over pure ZrO_2. However, heavy condensate products were obtained, like cyclic trimers and aromatics. The selectivity of the C_8 ketone increased dramatically when the reaction was conducted over 1% Cu–ZrO_2. It is believed that adding Cu on ZrO_2 facilitates the hydrogenation of the C=C bond in the α,β-unsaturated C_8 ketone immediately after the dimeric condensates form, preventing the dimer condensates from undergoing a conjugate addition with ketone enolates to produce heavy condensate products. Increasing the percentage of Cu supported on ZrO_2 from 1 wt % to 15 wt % does not have an important impact on the selectivity of the products, where the selectivity of the C_8 ketone was slightly decreased from 64% to 61%, with increasing the percentage of the copper loaded on the support along with the increased production of 2-butanol and the conversion of the C_8 ketone to C_8 alcohol. However, it is obvious that increasing this percentage leads to decreasing the conversion of MEK, probably because the hydrogenation of MEK is reversible. With more copper, MEK can be hydrogenated to 2-butanol, but then the 2-butanol can be dehydrogenated to MEK, as illustrated in Figure 7. This makes it look like less MEK was converted. The conversion of MEK and the main products selectivity are shown in Table 2.

Table 2. Catalytic activity for the conversion of methyl ethyl ketone (MEK) to a desirable product (C_8 ketone) over several catalysts.

Catalysts	Conv. of MEK (%)	Sel. of 2-Butanol (%)	Sel. of C_8 Ketone (%)	Sel. of C_8 Alcohol (%)	Others (%)
ZrO_2	26	0	5	0	95 [a]
1% Cu–ZrO_2	78	12	64	7	17 [b]
15% Cu–ZrO_2	63	18	61	6	15 [b]

[a] Others include MVK, unsaturated C_8 ketone, cyclic trimers condensate, and aromatics. [b] Others include MVK, C_{12} ketone, C_{12} alcohol, and condensation products.

2.2.5. Reaction of MEK over Different Metals Loaded on ZrO_2

Different metals (Cu, Ni, Pd, and Pt) supported on ZrO_2 were investigated in this work, in order to see the effect of the metal identity on the catalytic performance. The conversion of MEK and the selectivity of the main products' results gathered after 1 h from the reaction using 1.0 g of the catalyst are shown in Figure 8.

As seen in this figure, all four of the catalysts give similar results. All four produce 5-methyl-3-heptanone as the main product, with smaller amounts of 5-methyl-3-heptanol and 2-butanol. The main difference is in the conversion of MEK. Perhaps surprisingly, the conversion of MEK is highest on Ni–ZrO_2 and Cu–ZrO_2 (82% and 78%, respectively). Pt–ZrO_2 and Pd–ZrO_2, which would be expected to be the most active hydrogenation catalysts, both yield MEK conversion of ~65%.

We hypothesize that the trend in the MEK conversion is attributed to the metal hydrogenation activity, but not in the expected way. The reaction of MEK on these multifunctional catalysts is due to multiple reaction pathways, which is detailed in Scheme 1. The metal sites catalyze the MEK hydrogenation to 2-butanol, while the ZrO_2 support catalyzes the aldol condensation of MEK via an aldol reaction on the base sites to produce β-hydroxy ketone (5-methyl-5-hydroxy-3-heptanone), followed by dehydration the later on the acid sites to an α,β-unsaturated C_8 ketone (5-methyl-3-heptenone). Subsequently, the hydrogenation of the α,β-unsaturated C_8 ketone over metal sites produces the saturated C_8 ketone and, further, a C_8 alcohol. The hydrogenation of MEK to 2-butanol is believed to be reversible, and 2-butanol is not expected to be converted further to other products. For this reason, the lower MEK conversion noted for the Pt and Pd catalysts may actually represent a higher activity for those metals—they are more

active in converting MEK to 2-butanol, and 2-butanol back to MEK. The aldol condensation reaction on ZrO_2 is, therefore, decreased, and the ultimate C_8 ketone yield is decreased.

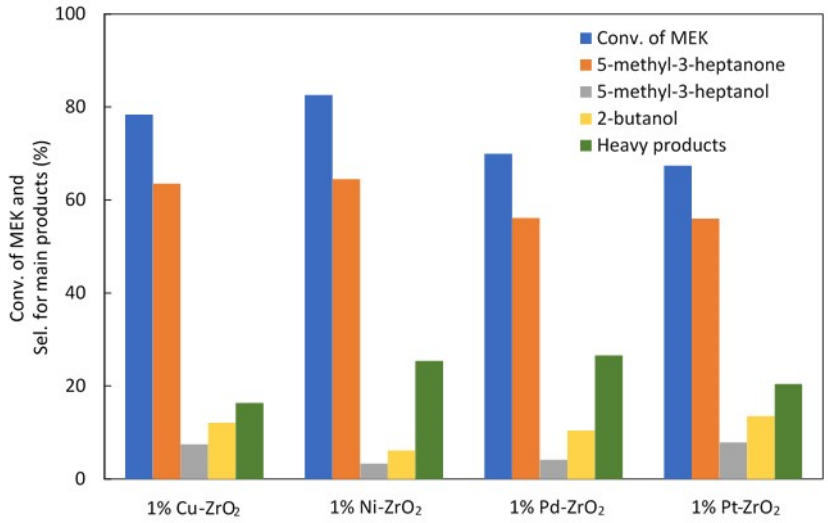

Figure 8. Catalytic results for the conversion of MEK to a variety of products over different catalysts. Reaction conditions: catalyst weight, 1.0 g; feed rate of MEK, 1.0 mL/h; H_2/MEK molar ratio, 2; reaction temperature, 180 °C; space time, 89 g mol^{-1} h. Heavy products include C_{12} ketone, C_{12} alcohol, condensation products, and so on.

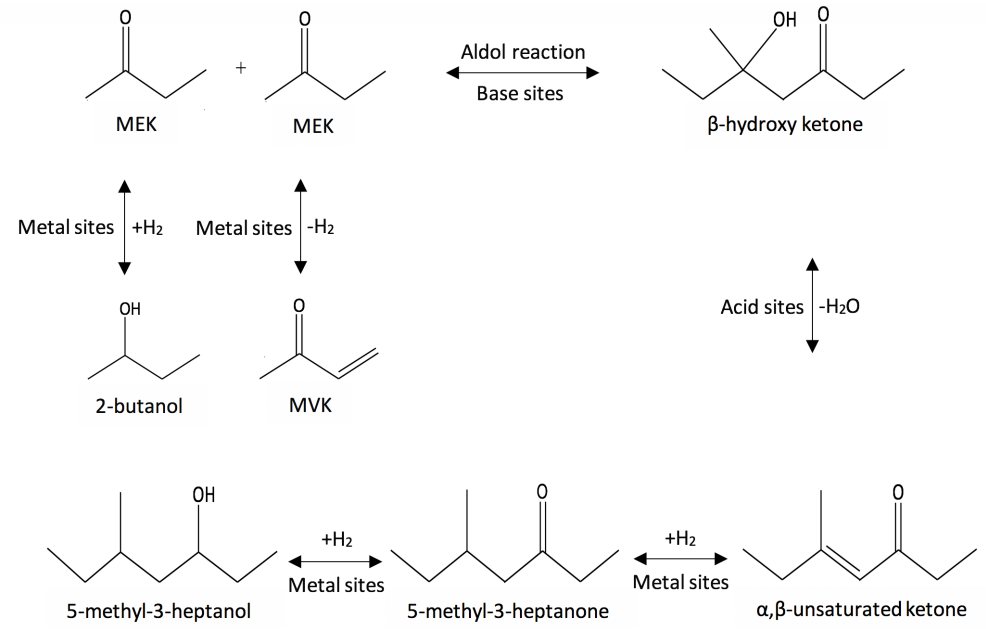

Scheme 1. The potential reaction pathways in the reaction of MEK to C_8 ketone and C_8 alcohol.

3. Materials and Methods

3.1. Materials

Methyl ethyl ketone, the copper precursor ((copper(II) nitrate tri-hydrate [$Cu(NO_3)_2{\cdot}3H_2O$ (99%)]), and the nickel precursor (nickel(II) nitrate hexahydrate [$Ni(NO_3)_2{\cdot}6H_2O$ (99%)]) were obtained from Fisher Scientific (Waltham, MA, USA), while the Pt precursor (tetraammineplatinum(II) nitrate [$Pt(NH_3)_4(NO_3)_2$]), Pd precursor (palladium(II) nitrate hydrate [$N_2O_6Pd{\cdot}xH_2O$]) and zirconium oxide (catalyst support, S.A 51 m^2/g, 1/8″ pellet) were obtained from Alfa Aesar (Haverhill, MA, USA).

3.2. Preparation of Supported Catalysts

All of the catalysts presented (Cu, Ni, Pd, and Pt supported on ZrO_2) were synthesized using an incipient wetness impregnation method. Before loading the metal, the support pellet was crushed and sieved to obtain particles < 0.15 mm in size (mesh 100). Next, a metal salt solution was prepared by dissolving the metal precursor in an amount of water just sufficient to fill the pores of an amount of the support. This solution was added to the support by dropwise addition, and was mixed thoroughly between the droplets. The catalyst was dried first in an oven overnight at 100 °C, then heated in a furnace at 110 °C for 2 h and calcined at 550 °C for 4 h in air. A ramp rate of 2 °C/min was used up to 110 °C and 1 °C/min up to 550 °C. After the calcination process, the catalyst was crushed and sieved to < 0.15 mm for all of the catalysts.

3.3. Catalytic Reaction

The catalytic conversion of MEK was performed in the gas phase in a continuous flow fixed-bed reactor made of stainless steel (ID = 0.85 cm) under atmospheric pressure. Before the reaction, a catalyst (1.0 g) was reduced in the reactor with flow rates of hydrogen and nitrogen equal to 68.5 and 16.5 mL/min, respectively, at 300 °C for 1 h, for Cu, Pd, and Pt supported ZrO_2, and at 500 °C for Ni–ZrO_2. After the reduction step, the MEK was mixed with hydrogen and nitrogen in a preheater at the desired reaction temperature prior to flowing into the reactor. The MEK was fed through the top of the reactor at a feed rate of 1 mL/h via a micro pump (Eldex 1SMP) (Napa, CA, USA), together with H_2 and N_2, with flow rates of 9.2 and 75.8 mL/min, respectively, and the molar ratio of H_2/MEK was 2. The reaction temperature was maintained at 180 °C. The product temperature effluent from the bottom of the reactor was maintained above 230 °C so as to avoid the condensation of liquid products. A product analysis was conducted using an on-line gas chromatograph (SRI 8610C) (Torrance, CA, USA) with an MXT-1 column (100% dimethyl polysiloxane (nonpolar phase), 60 m, ID 0.53 mm), and FID and TCD detectors for the analysis of hydrocarbons and oxygenates. The oven was held at 40 °C for 5 min, raised to 120 °C at a ramp rate of 40 °C/min, then raised to 250 °C at a rate of 20 °C/min, and held at this temperature for 10 min. An Agilent 7890A GC-MS system equipped with an Agilent 5975C MS detector (Santa Clara, CA, USA) was used to identify the products detected by the GC.

The conversion of MEK and the selectivity for the products were calculated using Equations (1) and (2), respectively, as follows:

$$\text{Conversion } \% = \frac{(\text{Moles of MEK})in - (\text{Mole of MEK})out}{(\text{Moles of MEK})in} \times 100 \quad (1)$$

$$\text{Selectivity } \% = \frac{(\text{Moles of product})}{(\text{Moles of total products})} \times 100 \quad (2)$$

3.4. Catalyst Characterization

3.4.1. X-ray Diffraction (XRD)

The X-ray diffraction patterns were obtained using a Rigaku Miniflex II desktop X-ray diffractometer (The Woodlands, TX, USA), using Cu K∝ radiation (λ = 0.15406 nm) at 30 kV and 15 mA. The scans of two theta angles were from 10° to 80° for all of the catalysts, with rate of 2°/min and a step size of 0.02°.

3.4.2. Temperature-Programed Reduction (H_2-TPR)

H_2-TPR was performed in an Altamira AMI-200 (Pittsburgh, PA, USA). In a typical experiment, 0.1 g of the sample was loaded in a quartz U-tube reactor, and argon was passed at 500 °C with a flow of 40 mL/min for an hour to pretreat the catalyst sample, followed by cooling to 50 °C. After treatment, the temperature was raised from 50 to 600 °C at a ramp rate of 10 °C/min, using H_2/Ar with flow of

40 mL/min (10 v/v%). The consumed H_2 as a function of the temperature was detected via a thermal conductivity detector (TCD).

3.4.3. Temperature-Programed Desorption (NH_3-TPD) and (CO_2-TPD)

The temperature programmed desorption of ammonia NH_3-TPD and carbon dioxide CO_2-TPD were performed on an Altamira AMI-200 system (Pittsburgh, PA, USA) in order to investigate the surface acidity and basicity of the catalysts. Before the NH_3-TPD studies, 0.1 g of a supported metal catalyst was loaded in a quartz U-tube reactor and was pretreated at 550 °C under helium for 1 h, followed by cooling to 100 °C. After that, the catalyst was reduced by passing H_2/Ar (10 v/v%) with a flow of 40 mL/min to 300 °C at a constant ramp rate of 10 °C/min and then held for 2 h, followed by cooling to 100 °C. After reducing the sample, 1% NH_3/He with a flow of 50 mL/min was then introduced at 100 °C for 1 h to saturate the sample with NH_3, and was subsequently flushed in a He flow at 100 °C for 2 h to remove the physically adsorbed ammonia molecules. Finally, the temperature was raised to 700 °C at a ramp rate of 10 °C/min. The CO_2-TPD was performed using the same instrument used in the NH_3-TPD measurements. Then, 0.1 g of the sample was preheated and reduced in the same series of steps as that described for NH_3-TPD, except that the cooling temperature after reducing the catalyst was 50 °C. After reducing, the sample was saturated with 10% CO_2 in helium with a flow of 50 mL/min at 50 °C, and was flushed with a He flow at 50 °C for 2 h to remove the physisorbed CO_2 molecules. Finally, the temperature was raised to 700 °C at a ramp rate of 10 °C/min. The desorbed NH_3 and CO_2 from the samples were detected by a thermal conductivity detector (TCD).

4. Conclusions

The conversion of MEK to 5-methyl-3-heptenone in one step has been demonstrated over 15% Cu–ZrO_2. The temperature and H_2/MEK molar ratio play a significant role in the selectivity of the products. The selectivity of the C_8 ketone increased with increasing the temperature, while at a lower temperature, the hydrogenation of MEK was favored, leading to the increased production of 2-butanol. In addition, it was found that with increasing the H_2/MEK molar ratio, the 2-butanol production increased, limiting the aldol condensation of MEK and decreasing the selectivity of C_8 ketone. Using 15% Cu–ZrO_2, the highest selectivity for C_8 ketone (~61%) was obtained at a 180 °C and H_2/MEK molar ratio of 2. Also, the results showed that using Cu–ZrO_2 at low loading of Cu (1 wt %) led to an increase in the conversion of MEK and a higher selectivity for the C_8 ketone. The catalytic results were similar for four of the different supported metals (Cu, Ni, Pd, and Pt) supported on ZrO_2 under the optimum operation conditions (at 180 °C and H_2/MEK molar ratio of 2), suggesting that all of the metals catalyze the same catalytic routes in obtaining 5-methyl-3-heptenone as the main product. However, the conversion of MEK was the highest on 1% Ni–ZrO_2 and 1% Cu–ZrO_2 (82% and 78%, respectively), with selectivity reaching 64%.

Author Contributions: Z.A. and H.A. conceived and designed the experiments; Z.A. performed the experiments; Z.A. analyzed the data; Z.A. wrote the paper; K.H. is the supervisor; K.H. and Z.A. interpreted the results; K.H. reviewed and edited the paper.

Funding: This research was funded by [the Higher Committee for Education Development in Iraq (HCED)] grant number [D-11-11], and [the Navy SBIR Phase II] [Contr #NG8335], in collaboration with [TekHolding, Inc.].

Conflicts of Interest: The authors declare no conflicts of interest.

References

1. Yoshikawa, N.; Yamada, Y.M.A.; Das, J.; Sasai, H.; Shibasaki, M. Direct catalytic asymmetric aldol reaction. *J. Am. Chem. Soc.* **1999**, *121*, 4168–4178. [CrossRef]
2. Roelofs, J.; van Dillen, A.J.; Jong, K.P. De Base-catalyzed condensation of citral and acetone at low temperature using modified hydrotalcite catalysts. *Catal. Today* **2000**, *60*, 297–303. [CrossRef]
3. Di Cosimo, J.I.; Diez, V.K.; Apesteguía, C.R. Base catalysis for the synthesis of α,β-unsaturated ketones from the vapor-phase aldol condensation of acetone. *Appl. Catal. A Gen.* **1996**, *137*, 149–166. [CrossRef]

4. Nielsen, A.T.; Houlihan, W.J. The aldol condensation. *Org. React.* **1968**, *16*, 2–3.
5. Kelly, G.J. Aldol Condensation Reaction and Catalyst Therefor. U.S. Patent No. 6,706,928, 16 March 2004.
6. Melo, L.; Giannetto, G.; Alvarez, F.; Magnoux, P.; Guisnet, M. Effect of the metallic/acid site (nPt/nA) ratio on the transformation of acetone towards methyl isobutyl ketone. *Catal. Lett.* **1997**, *44*, 201–204. [CrossRef]
7. Reichle, W.T. Catalytic Aldol Condensations. U.S. Patent No. 4,165,339, 21 August 1979.
8. Vannice, M.A.; Sen, B. Metal-support effects on the intramolecular selectivity of crotonaldehyde hydrogenation over platinum. *J. Catal.* **1989**, *115*, 65–78. [CrossRef]
9. Claus, P. Selective hydrogenation of ά,β-unsaturated aldehydes and other C=O and C=C bonds containing compounds. *Top. Catal.* **1998**, *5*, 51–62. [CrossRef]
10. Zhu, L.; Lu, J.Q.; Chen, P.; Hong, X.; Xie, G.Q.; Hu, G.S.; Luo, M.F. A comparative study on Pt/CeO_2 and Pt/ZrO_2 catalysts for crotonaldehyde hydrogenation. *J. Mol. Catal. A Chem.* **2012**, *361*, 52–57. [CrossRef]
11. Gallezot, P.; Richard, D. Selective hydrogenation of α,β-unsaturated aldehydes. *Catal. Rev.* **1998**, *40*, 81–126. [CrossRef]
12. Mohr, C.; Claus, P. Hydrogenation properties of supported nanosized gold particles. *Sci. Prog.* **2001**, *84*, 311–334. [CrossRef]
13. Sul'man, E. Selective hydrogenation of unsaturated ketones and acetylene alcohols. *Russ. Chem. Rev.* **1994**, *63*, 923–936. [CrossRef]
14. Szöllősi, G.; Mastalir, A.; Molnár, Á.; Bartók, M. Hydrogenation of α,β-unsaturated ketones on metal catalysts. *React. Kinet. Catal. Lett.* **1996**, *57*, 29–36. [CrossRef]
15. Ravasio, N.; Antenori, M.; Gargano, M.; Rossi, M. Chemoselectivity and regioselectivity in the hydrogenation of α,β-unsaturated carbonyl compounds promoted by Cu/Al_2O_3. *J. Mol. Catal.* **1992**, *74*, 267–274. [CrossRef]
16. Ravasio, N.; Antenori, M.; Gargano, M.; Mastrorilli, P. $CuSiO_2$: An improved catalyst for the chemoselective hydrogenation of α,β-unsaturated ketones. *Tetrahedron Lett.* **1996**, *37*, 3529–3532. [CrossRef]
17. Molnár, Á.; Bucsi, I.; Bartók, M. Pinacol Rearrangement on Zeolites. *Stud. Surf. Sci. Catal.* **1988**, *41*, 203–210.
18. Multer, A.; McGraw, N.; Hohn, K.; Vadlani, P. Production of methyl ethyl ketone from biomass using a hybrid biochemical/catalytic approach. *Ind. Eng. Chem. Res.* **2012**, *52*, 56–60. [CrossRef]
19. Emerson, R.R.; Flickinger, M.C.; Tsao, G.T. Kinetics of dehydration of aqueous 2,3-butanediol to methyl ethyl ketone. *Ind. Eng. Chem. Prod. Res. Dev.* **1982**, *21*, 473–477. [CrossRef]
20. Zhang, W.; Yu, D.; Ji, X.; Huang, H. Efficient dehydration of bio-based 2,3-butanediol to butanone over boric acid modified HZSM-5 zeolites. *Green Chem.* **2012**, *14*, 3441–3450. [CrossRef]
21. Bucsi, I.; Molnár, Á.; Bartók, M.; Olah, G.A. Transformation of 1,2-diols over perfluorinated resinsulfonic acids (Nafion-H). *Tetrahedron* **1994**, *50*, 8195–8202. [CrossRef]
22. Török, B.; Bucsi, I.; Beregszászi, T.; Kapocsi, I.; Molnár, Á. Transformation of diols in the presence of heteropoly acids under homogeneous and heterogeneous conditions. *J. Mol. Catal. A Chem.* **1996**, *107*, 305–311. [CrossRef]
23. Nikitina, M.A.; Ivanova, I.I. Conversion of 2,3-Butanediol over Phosphate Catalysts. *ChemCatChem* **2016**, *8*, 1346–1353. [CrossRef]
24. Lee, J.; Grutzner, J.B.; Walters, W.E.; Delgass, W.N. The conversion of 2,3-butanediol to methyl ethyl ketone over zeolites. *Stud. Surf. Sci. Catal.* **2000**, *130*, 2603–2608.
25. Yu, E.K.; Saddler, J.N. Fed-batch approach to production of 2,3-butanediol by Klebsiella pneumoniae grown on high substrate concentrations. *Appl. Environ. Microbiol.* **1983**, *46*, 630–635. [PubMed]
26. Zeng, A.P.; Biebl, H.; Deckwer, W.D. Effect of pH and acetic acid on growth and 2,3-butanediol production of Enterobacter aerogenes in continuous culture. *Appl. Microbiol. Biotechnol.* **1990**, *33*, 485–489. [CrossRef]
27. Mas, C. De; Jansen, N.B.; Tsao, G.T. Production of optically active 2,3-butanediol by Bacillus polymyxa. *Biotechnol. Bioeng.* **1988**, *31*, 366–377. [CrossRef] [PubMed]
28. Ledingham, G.A.; Neish, A.C. *Fermentative Production of 2.3 Butanediol Industrial Fermentations*; Underkofler, L.A., Hickey, R.J., Eds.; Chemical Publishing Co: New York, USA, 1954; Volume 2, pp. 27–93.
29. Jansen, N.B.; Flickinger, M.C.; Tsao, G.T. Production of 2,3-butanediol from D-xylose by Klebsiella oxytoca ATCC 8724. *Biotechnol. Bioeng.* **1984**, *26*, 362–369. [CrossRef] [PubMed]
30. Qureshi, N.; Cheryan, M. Effects of aeration on 2,3-butanediol production from glucose by Klebsiella oxytoca. *J. Ferment. Bioeng.* **1989**, *67*, 415–418. [CrossRef]
31. Ji, X.J.; Huang, H.; Du, J.; Zhu, J.G.; Ren, L.J.; Hu, N.; Li, S. Enhanced 2,3-butanediol production by Klebsiella oxytoca using a two-stage agitation speed control strategy. *Bioresour. Technol.* **2009**, *100*, 3410–3414. [CrossRef]

32. Saha, B.C.; Bothast, R.J. Production of 2,3-butanediol by newly isolated Enterobacter cloacae. *Appl. Microbiol. Biotechnol.* **1999**, *52*, 321–326. [CrossRef]
33. Hattori, H. Heterogeneous basic catalysis. *Chem. Rev.* **1995**, *95*, 537–558. [CrossRef]
34. Yamaguchi, T.; Nakano, Y.; Iizuka, T.; Tanabe, K. Catalytic activity of ZrO_2 and ThO_2 for HD exchange reaction between methyl group of adsorbed isopropyl alcohol-d8 and surface OH group. *Chem. Lett.* **1976**, 677–678. [CrossRef]
35. Chary, K.V.R.; Sagar, G.V.; Srikanth, C.S.; Rao, V.V. Characterization and catalytic functionalities of copper oxide catalysts supported on zirconia. *J. Phys. Chem. B* **2007**, *111*, 543–550. [CrossRef]
36. Sagar, G.V.; Rao, P.V.R.; Srikanth, C.S.; Chary, K.V.R. Dispersion and Reactivity of Copper Catalysts Supported on Al_2O_3–ZrO_2. *J. Phys. Chem. B* **2006**, *110*, 13881–13888. [CrossRef] [PubMed]
37. Van der Grift, C.J.G.; Mulder, A.; Geus, J.W. Characterization of silica-supported copper catalysts by means of temperature-programmed reduction. *Appl. Catal.* **1990**, *60*, 181–192. [CrossRef]
38. Shimokawabe, M.; Asakawa, H.; Takezawa, N. Characterization of copper/zirconia catalysts prepared by an impregnation method. *Appl. Catal.* **1990**, *59*, 45–58. [CrossRef]
39. Dow, W.P.; Wang, Y.P.; Huang, T.J. Yttria-stabilized zirconia supported copper oxide catalyst: I. Effect of oxygen vacancy of support on copper oxide reduction. *J. Catal.* **1996**, *160*, 155–170. [CrossRef]
40. Robertson, S.D.; McNicol, B.D.; De Baas, J.H.; Kloet, S.C.; Jenkins, J.W. Determination of reducibility and identification of alloying in copper-nickel-on-silica catalysts by temperature-programmed reduction. *J. Catal.* **1975**, *37*, 424–431. [CrossRef]
41. Li, Z.; Hu, X.; Zhang, L.; Liu, S.; Lu, G. Steam reforming of acetic acid over Ni/ZrO_2 catalysts: Effects of nickel loading and particle size on product distribution and coke formation. *Appl. Catal. A Gen.* **2012**, *417*, 281–289. [CrossRef]
42. Roh, H.S.; Jun, K.W.; Dong, W.S.; Chang, J.S.; Park, S.E.; Joe, Y.I. Highly active and stable Ni/Ce–ZrO_2 catalyst for H_2 production from methane. *J. Mol. Catal. A Chem.* **2002**, *181*, 137–142. [CrossRef]
43. Song, Y.Q.; Liu, H.M.; He, D.H. Effects of hydrothermal conditions of ZrO_2 on catalyst properties and catalytic performances of Ni/ZrO_2 in the partial oxidation of methane. *Energy Fuels.* **2010**, *24*, 2817–2824. [CrossRef]
44. Sun, L.; Tan, Y.; Zhang, Q.; Xie, H.; Han, Y. Tri-reforming of coal bed methane to syngas over the Ni-Mg-ZrO_2 catalyst. *J. Fuel Chem. Technol.* **2012**, *40*, 831–837. [CrossRef]
45. Chen, S.; Luo, L.; Cheng, X. Influence of preparation method on the performance of Pd/ZrO_2-Al_2O_3 catalysts for HDS. *Indian J. Chem. Technol.* **2009**, *16*, 272–277.
46. Ivanova, A.S.; Slavinskaya, E.M.; Gulyaev, R.V.; Zaikovskii, V.I.; Stonkus, O.A.; Danilova, I.G.; Plyasova, L.M.; Polukhina, I.A.; Boronin, A.I. Metal–support interactions in Pt/Al_2O_3 and Pd/Al_2O_3 catalysts for CO oxidation. *Appl. Catal. B Environ.* **2010**, *97*, 57–71. [CrossRef]
47. Lee, H.C.; Lee, D.; Lim, O.Y.; Kim, S.; Kim, Y.T.; Ko, E.Y.; Park, E.D. ZrO_2-supported Pt catalysts for water gas shift reaction and their non-pyrophoric property. *Stud. Surf. Sci. Catal.* **2007**, *167*, 201–206.
48. Kozlowski, J.T.; Davis, R.J. Heterogeneous catalysts for the Guerbet coupling of alcohols. *ACS Catal.* **2013**, *3*, 1588–1600. [CrossRef]
49. Gabriëls, D.; Hernández, W.Y.; Sels, B.; Van Der Voort, P.; Verberckmoes, A. Review of catalytic systems and thermodynamics for the Guerbet condensation reaction and challenges for biomass valorization. *Catal. Sci. Technol.* **2015**, *5*, 3876–3902. [CrossRef]